Analysis of loss mechanisms and coherence times of the ALQ

Author	Affiliation	Email
Alfredo Levy Yeyati	UAM	a.l.yeyati@uam.es
Project Number	Project Start Date	Duration
828948	01.04.2019	48 Months
Classification		
	PU	
File Name		
AndQC_WP5_D5_1.pdf		
WP No	Work Package Name	
5	Supporting theory	
Deliverable No	Deliverable Name	
D5.1	Analysis of loss mechanisms and coherence times of the ALQ	
	Approved by	
	Steering Committee of the action	

The opinions expressed in the document are of the authors only and no way reflect the European Commission's opinions. The European Union is not liable for any use that may be made of the information. This project has received funding from the European Union's Horizon 2020 research and innovation programme under grant agreement No 828948.

DOCUMENT REVISION HISTORY

Revision	Date	Description	Author
1.0	31.03.2020		Alfredo Levy Yeyati

Table of Contents

1. Introduction

While experiments in semiconducting nanowire Josephson junctions are rapidly progressing [1-4] the available data on the coherent dynamics of Andreev levels in such devices is still limited. In contrast, we have now a fair amount of data obtained on superconducting atomic contacts In the one atom limit these systems are typically characterized by a single well transmitted channel hosting a pair Andreev bound states which can be populated with zero, one or two quasiparticles, leading to three many body states |g>, |o> and |e> [5]. The core of the analysis presented in this report is based on recent experiments from the Saclay group using a circuit QED set up similar to that of Ref. [5] but including a quantum limited amplifier, based on a Josephson Parametric Converter (JPC) [6], which allows for an improved resolution. These new data provide valuable information on the basic loss and decoherence mechanisms for Andreev level qubits (ALQs).

2. New experimental data

The Saclay group has performed continuous measurements of the quasiparticle occupation of the Andreev states in atomic point contacts using the setup illustrated in Fig. 1. Atomic contacts were obtained by elongating a suspended aluminum bridge on a flexible substrate. The bridge is part of a 100 μm x 20 μm aluminum loop, placed at the shorted end of a quarter-wavelength coplanar wave-guide resonator with bare frequency f_R=8.77 GHz. A magnetic flux threading the loop controls the superconducting phase difference ϕ across the contact. The actual resonance frequency of the resonator encodes the state of the ALQ in the contact. A weak microwave tone at frequency f_R is sent into the resonator and the reflected signal is amplified first by a JPC placed at the mixing chamber, then by a HEMT at 1.2K. After homodyne mixing, one obtains the in-phase (I) and out-of phase (Q) quadratures of the reflected signal,. The microwave resonator was characterized while the bridge was open, leading to a total photon decay rate $\kappa/2\pi$= 9.5μs^{-1}. When a contact is formed, time-domain measurements are used to perform the spectroscopy of the Andreev levels in the contact, i.e. to determine the transition frequency $f_A(\phi)$ between the even states.

The results in Fig. 2 illustrate the continuous measurements of I and Q for a contact with f_A (π)= 6.33GHz. Three blobs are visible in a density plot of the values of (I, Q), corresponding to the states |g>, |o> and |e> of a contact having just a single low-energy Andreev state. The identification of the blobs is achieved from the time-domain measurements. By analyzing simultaneously the traces I(t) and Q(t) with a hidden Markov model [7], the transition rates between the 3 states can be inferred. To account for the spin degeneracy of the odd state |o>, the rate from |g> (or |e>) to |o> is taken as twice the rate from |g> (or |e>) to |oσ>, where σ denotes either spin direction. The 10 resulting rates from i to j (labeling states within |g>, |o↑>, |o↓> or |e>) are denoted as Γ_{ij}. In most of the measurements, it is found that within experimental accuracy $\Gamma_{go\sigma} = \Gamma_{o\sigma e}$ and $\Gamma_{eo\sigma} = \Gamma_{o\sigma g}$. The corresponding processes are, respectively, the addition and the removal of one quasiparticle in the Andreev level. The approximate equality of the rates suggests that there are no charging effects.

One can therefore define $\Gamma_{in} \equiv \Gamma_{go\sigma}$ and $\Gamma_{out} \equiv \Gamma_{o\sigma g}$ [8]. To make the notations more explicit, the excitation and relaxation rates in the even manifold are denoted $\Gamma_{exc} \equiv \Gamma_{ge}$ and $\Gamma_{rel} \equiv \Gamma_{eg}$.

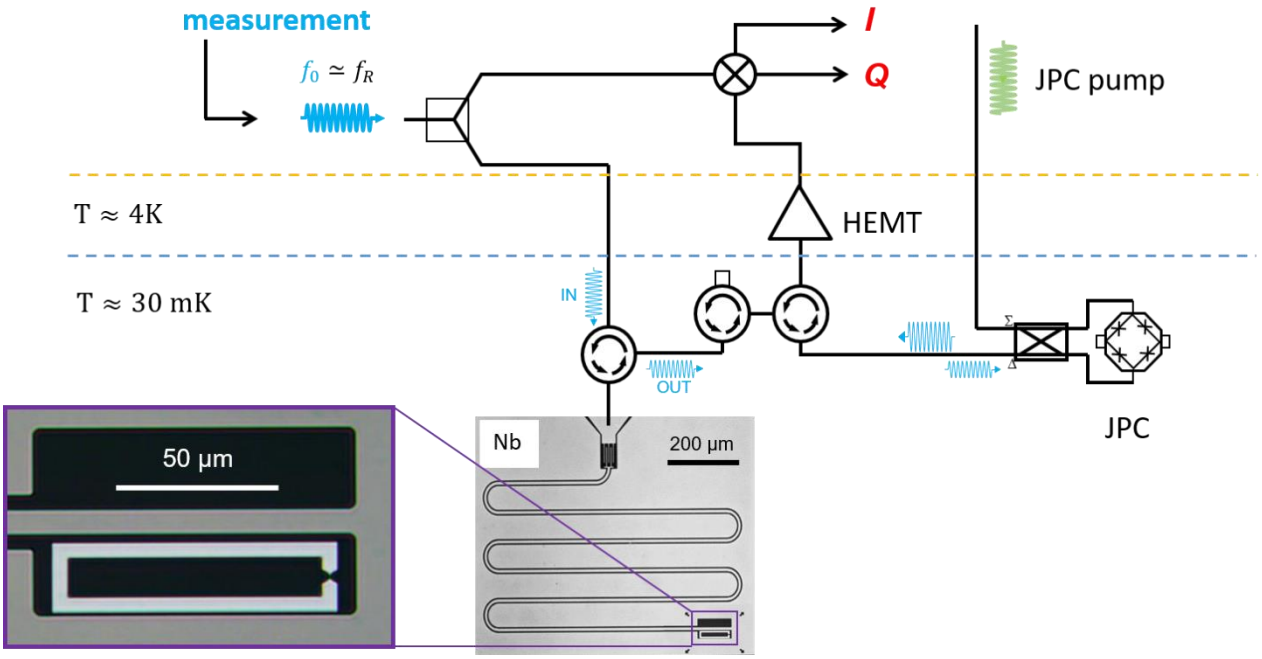

Fig. 1: Schematics of the setup used for continuous monitoring of the Andreev states population in an atomic contact.

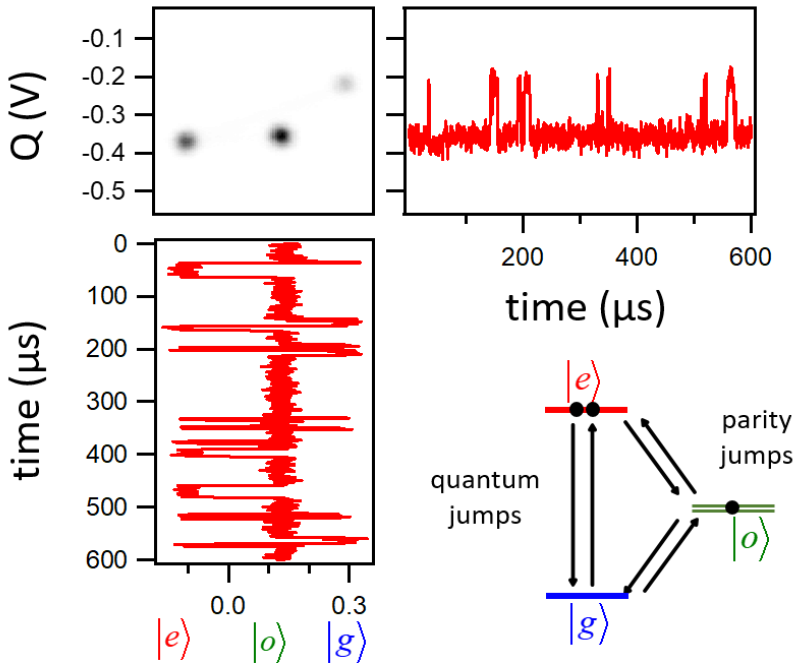

Fig 2: Quadratures I and Q of the reflected signal as a function of time measured on the atomic contact with Andreev frequency $f_A(\pi)$=6.33 GHz and a measurement power corresponding to $\langle n_{g,e} \rangle$=220 photons in the resonator. The phase difference ϕ is fixed at π. The upper-left panel shows a density plot of values of I and Q in a 0.8 ms time interval.

We find that, in general, the transition rates depend on the intensity of the probe tone at f_R. This intensity can be expressed in terms of the average number of photons in the cavity n, which characterizes the Poisson distribution in the driven cavity. It is important to notice that n depends also on the parity of the occupation of the Andreev levels, so that $n_{g,e}=n_0/(1+(2\chi/\kappa)^2)$, where χ is the cavity pull (or shift in the resonator frequency) when the system is in the |g> or |e> state. The number of photons is calibrated by measuring the Stark shift of the cavity and the cavity pull at a given power. The variation of the rates and the states populations with the mean number of photons is illustrated in Fig. 3 for the same contact as in Fig. 2.

As can be observed, while Γ_{in} and Γ_{out} remain roughly constant, Γ_{exc} and Γ_{rel} exhibit a strong variation with n. At large number of photons there is an inversion of population in the even manifold while the odd states population remains roughly constant.

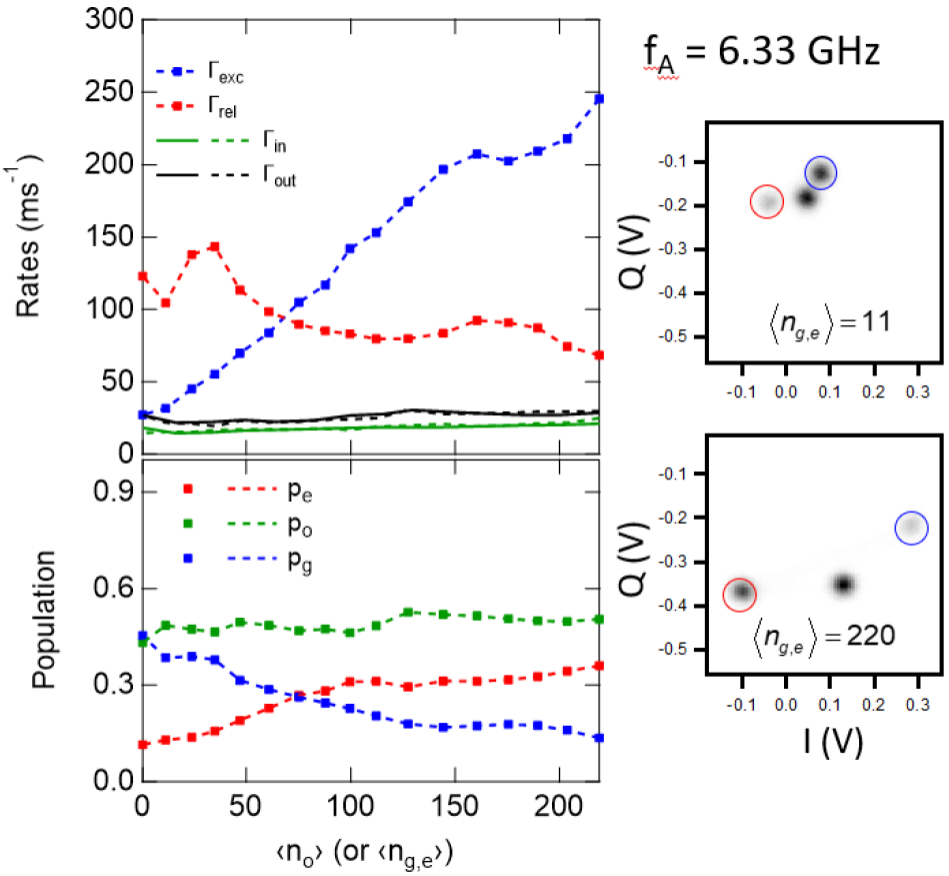

Fig. 3: Rates and population dependence on the mean number of photons in the cavity.

In order to extract information on the intrinsic dynamics of the Andreev qubit, the rates in the limit $n \to 0$ were determined for several contacts at phase π.The results are collected in Fig. 4.

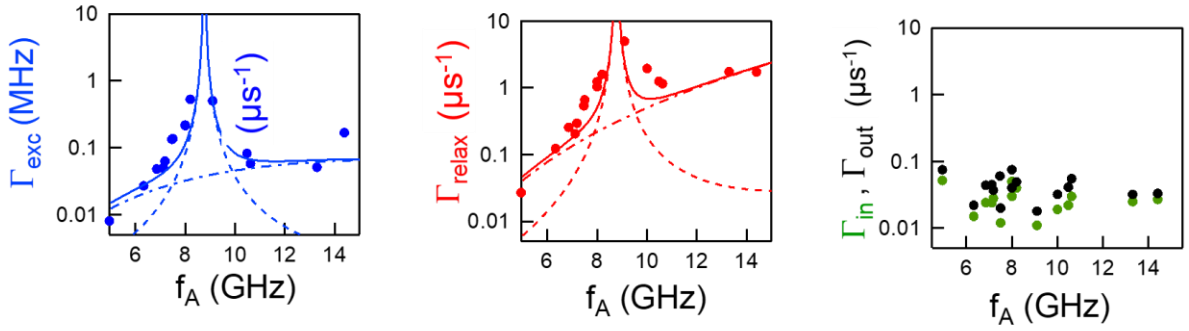

Fig 4: Frequency dependence of the rates obtained for several contacts with different f_A (at $\phi=\pi$).

3. Theoretical analysis

Two main sources for relaxation and decoherence have been pointed out for atomic contact ALQs: the coupling to photons in the electromagnetic environment (EM) and the emission or absorption of phonons in the leads. The first one has been analyzed in Ref. [9], where the relation between Γ_{exc} and Γ_{rel} with the environmental impedance $Z(\omega)$ was derived by considering the effect of phase fluctuations, leading to the following Purcell rate

$$\Gamma_P^0 = \frac{\pi}{2h}\frac{Z(f_A)}{R_Q}\frac{(1-\tau)\left(\tau\sin^2\frac{\phi}{2}\right)^2}{\left(1-\tau\sin^2\frac{\phi}{2}\right)^{\frac{3}{2}}},$$

where τ is the contact transmission and R_Q is the quantum of resistance ($h/2e^2$). Assuming that the EM environment is in thermal equilibrium Γ_{exc} and Γ_{rel} are related to Γ_P^0 by $\Gamma_{rel} = \Gamma_P^0(1+N_{BE}(T_{env}))$ and $\Gamma_{exc} = \Gamma_P^0 N_{BE}(T_{env})$, where $N_{BE}(T_{env})$ is the Bose factor at the environmental temperature T_{env}. The dashed lines in the plots for Γ_{exc} and Γ_{rel} in Fig. 4 correspond to values calculated assuming T_{env}=200mK, i.e. significantly larger than the measured temperature of the mixing chamber in the experiment. Still, the effect of the environment accounts only for the relaxation and excitation rates close to f_R. In addition to the resonance around f_R, the relaxation rates displays a background that increases rapidly with f_A. One can associate this background with phonon emission or absorption, with a rate proportional to f_A^4, as shown by the dash-dotted line in the plots for Γ_{exc} and Γ_{rel} in Fig. 4. Note however, that the amplitude of the proportionality prefactor required to reach a good agreement with the experimental data is ~300 larger than expected from electron-phonon interaction in aluminium wires [10]. While such enhancement might be due to the reduced dimensionality in the bridge region, a detailed theory for this effect is still lacking.

On the other hand, the rates Γ_{in} and Γ_{out} correspond to processes that change the parity and involve quasiparticles in the continuum with energy E_{qp} larger than the superconducting gap [11]. The transition |g>→|o> corresponds to a quasiparticle at E_{qp} that relaxes into the Andreev, with the emission of a photon or a phonon at E_{qp}-E_A. The reverse process involves the recombination of a quasiparticle at E_{qp} with the one in the Andreev level, and the emission of a photon or phonon at E_{qp}+E_A. Altogether one predicts $\Gamma_{in} \sim f(E_{qp})D(E_{qp}-E_A)$ and $\Gamma_{out} \sim f(E_{qp})D(E_{qp}+E_A)$, where $f(E_{qp})$ is the Fermi factor corresponding to the occupation of the quasiparticle state and $D(E)$ the density of states for the bosonic modes. The observation $\Gamma_{in} < \Gamma_{out}$ corresponds to $D(E)$ being an increasing function of E, which is expected for phonons. As expected, the number of photons in the cavity plays no role in these processes. The fluctuations of the rates from one measurement to another indicate that the

density of quasiparticles in the continuum varies at time scales of hours or days in an uncontrolled manner.

Finally, we discuss the dependence of Γ_{exc} and Γ_{rel} with the number of photons in the resonator. Such dependence has been predicted in Ref. [12] in a theory that the authors named “dressed dephasing”. They consider first a qubit without resonator (bare qubit), with eigenstates $|g_0\rangle$ and $|e_0\rangle$, coupled to classical fluctuators that only cause fluctuations in its transition frequency (σ_z coupling), and hence pure dephasing. When coupled to a resonator the eigenstates become “dressed” states $|g,n\rangle$ and $|e,n\rangle$, which are rotated with respect to the bare ones. As a consequence, the fluctuators acquire a transverse amplitude in the new basis and also cause relaxation/excitation in addition to dephasing. Similarly, the transverse coupling that cause relaxation to the bare qubit at a rate Γ^0_{rel} are reduced in the rotated basis. The predictions of Ref. [12] can be written as

$$\Gamma^n_{rel} = \Gamma^0_{rel}(1-\nu) + \Gamma^n_P + \alpha^2 S(\Delta)\nu\,; \quad \Gamma^n_{exc} = \alpha^2 S(-\Delta)\nu$$

where Γ^n_P is the Purcell rate, $\Delta = f_A - f_R$ is the qubit-cavity detuning, $\nu = (n/n_{crit})$ where $n_{crit} = \Delta/2\chi$ and $S(\omega)$ is the noise spectrum for the fluctuators. At finite temperature, the first two terms in Γ^n_{rel} are multiplied by $1+N_{BE}(T_{env})$ and appear in Γ^n_{exc} with a factor $N_{BE}(T_{env})$. A direct comparison of this theory with the data is still pending.

As a complementary approach, we have performed numerical simulations of the system dynamics described by a master equation with a coherent part and a dissipative part having the Lindblad form

$$\partial_t \rho = -i[H,\rho] + \mathcal{L}_D\,\rho$$

where $H = H_A + H_{env} + H_{eA} + H_d$, with

$$H_A = \sum_{\nu=\pm} \nu E_A \gamma_\nu^+ \gamma_\nu\,;\; H_{env} = h f_R a^+ a\,;\; H_{eA} = \frac{\lambda f_R}{\sqrt{2Z}} \sum_{\nu,\nu'} I_{\nu\nu'} \gamma_\nu^+ \gamma_{\nu\nu'}(a + a^+)\,; H_d = g_{drive}(a\, e^{i\omega_d t} + a^+ e^{-i\omega_d t})$$

Associated respectively to the Andreev states, the resonator, the coupling between the ABSs and the resonator and the driving field Hamiltonians. Notice that $I_{\nu\nu'}$ denote the current matrix elements between the ABSs, which have been derived in previous works [13]. On the other hand, the dissipative part is divided as $\mathcal{L}_D\,\rho = \mathcal{L}_p\,\rho + \mathcal{L}_q\,\rho$, corresponding to the parity and quantum jumps respectively, given by

$$\mathcal{L}_p\,\rho = \tfrac{1}{2}\textstyle\sum_\nu \Gamma_{in}(2\gamma_\nu^+\rho\gamma_\nu - \gamma_\nu\gamma_\nu^+\rho - \rho\gamma_\nu^+\gamma_\nu) + \Gamma_{out}(2\gamma_\nu\rho\gamma_\nu^+ - \gamma_\nu^+\gamma_\nu\rho - \rho\gamma_\nu\gamma_\nu^+)$$

$$\mathcal{L}_q\,\rho = \tfrac{1}{2}[\Gamma_{rel}(2a\rho a^+ - a^+a\rho - \rho a^+a) + \Gamma_{\rm exc}(2a^+\rho a - aa^+\rho - \rho a\, a^+)]$$

We assume that the rates Γ_{in} and Γ_{out} are fixed at constant values as suggested by the experimental results, while Γ_{rel} and $\Gamma_{\rm exc}$ correspond to the Purcell rates. The master equation can be solved easily using the rotated wave approximation (RWA), valid for small qubit-resonator detuning. The results for the states occupation as a function of the driving intensity g and different values of f_A and f_R are illustrated in Fig. 5. When plotted as a function of the mean number of photons (lower panels in Fig. 5) the states population exhibit a similar behaviour as the one found for the data in Fig. 3, i.e. that the odd states population remains rather constant while the ground (excited) state population decrease (increase) with the number of photons. Although not shown in these plots, the population of the states in the even sector tends to cross for ~ 60 photons, in qualitative agreement with the experimental data.

4. Conclusions

Coupling to microwave photons in the resonator and phonons in the leads forming the contact have been identified as the main mechanisms leading to relaxation and parity jumps in an ALQ defined on atomic point contacts. The relaxation and excitation rates were found to depend strongly on the number of photons in the resonator which can lead to an inversion of the steady state population in the even sector. In contrast, the rates associated to parity jumps remain almost constant with increasing number of photons, although exhibiting large fluctuations. Our theoretical analysis accounts quantitatively for the frequency dependence of the relaxation and excitation rates in the limit of zero photons and close to the resonator frequency. Beyond this frequency range the rates are well described as being due to phonon emission or absorption, although rather large values of the electron-phonon coupling parameter has to be assumed. Regarding the dependence with the number of photons, a detailed comparison with the theory of "dressed dephasing" in Ref. [12] is still pending but we have shown that the observed behaviour of the states population can be well described by a simple master Lindblad equation for the Andreev states coupled to a driven resonator. On the other hand, a description of the rates associated to parity jumps in the lines of Ref. [11] was found adequate but the origin of excess quasiparticles remains to be understood.

Finally, let us comment that we expect to be able to perform a similar analysis for the case of ALQs defined on semiconducting nanowires junctions. Theoretical work in this direction will be in parallel with the experimental progress within the consortium.

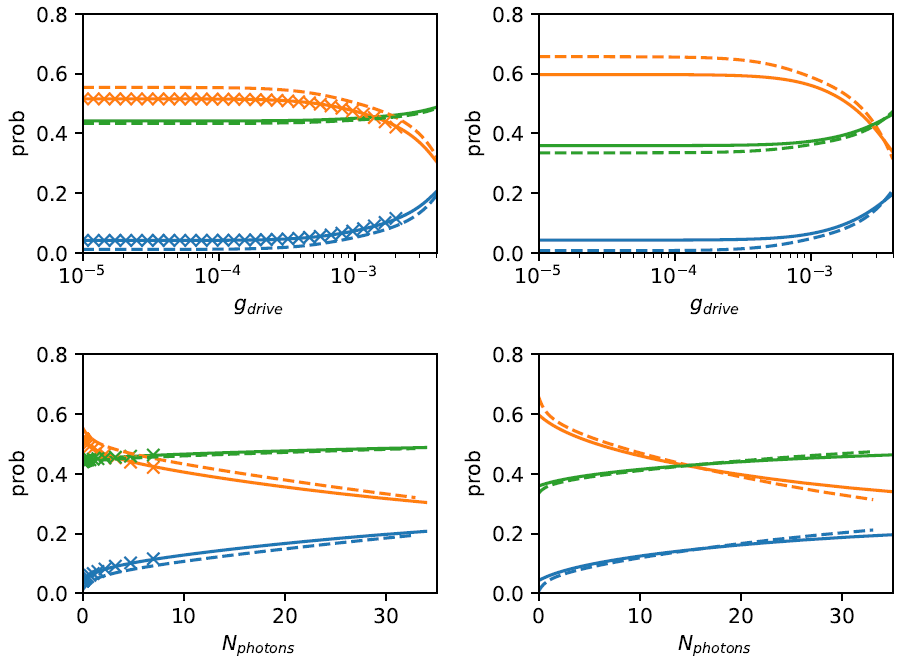

Fig. 5: upper panels: population of the ground (orange), odd (green) and excited (blue) states as a function of the driving intensity for f_A=0.2Δ_S (left) and f_A=0.448Δ_S (right). The full and dashed lines correspond to f_R=1.1f_A and f_R=1.01f_A respectively. The crosses correspond to the exact (non-RWA) calculation. Lower panels: same results as a function of the mean number of photons. Parameters: λ=0.01, $\Gamma_{in} = 3.1 \times 10^{-5}\Delta_S$, $\Gamma_{out} = 5.1 \times 10^{-5}\Delta_S$, all energies in units of the superconducting gap Δ_s.

5. References

[1] D. J. van Woerkom, A. Proutski, B. van Heck, D. Bouman, J.I. Väyrynen, L. I. Glazman, P. Krogstrup, J. Nygård, L. P. Kouwenhoven and A. Geresdi, Microwave spectroscopy of spinful Andreev bound states in ballistic semiconductor Josephson junctions, Nature Phys 13, 876 (2017).

[2] M. Hays, G. de Lange, K. Serniak, D. J. van Woerkom, D. Bouman, P. Krogstrup, J. Nygård, A. Geresdi, and M. H. Devoret, Direct Microwave Measurement of Andreev-Bound-State Dynamics in a Semiconductor-Nanowire Josephson Junction, Phys. Rev. Lett. 121, 047001 (2018).

[3] L. Tosi, C. Metzger, M.F. Goffman, C. Urbina, H. Poth-ier, Sunghun Park, A. Levy Yeyati, J. Nygard, and P.Krogstrup, Spin-orbit splitting of Andreev states revealed by microwave spectroscopy, Phys. Rev. X 9, 011010 (2019).

[4] M. Hays, V. Fatemi, K. Serniak, D. Bouman, S. Dia-mond, G. de Lange, P. Krogstrup, J. Nygrd, A. Geresdi,M. H. Devoret, “Continuous monitoring of a trapped,superconducting spin”, arXiv:1908.02800.

[5] C. Janvier, L. Tosi, L. Bretheau, Ç.O. Girit, M. Stern, P. Bertet, P. Joyez, D. Vion, D. Esteve, M. F. Goffman, H. Pothier, and C. Urbina, Coherent manipulation of Andreev states in superconducting atomic contacts, Science **349**, 1199 (2015).

[6] N. Bergeal, F. Schackert, M. Metcalfe, R. Vijay, V. E. Manucharyan, L. Frunzio, D. E. Prober, R. J. Schoelkopf, S. M. Girvin, and M. H. Devoret, Phase-preserving amplification near the quantum limit with a Josephson ring modulator, Nature **465**, 64 (2010).

[7] M. Greenfeld, D.S. Pavlichin, H. Mabuchi, and D. Herschlag, Single Molecule Analysis Research Tool (SMART): An Integrated Approach for Analyzing Single Molecule Data. PLoS ONE **7**, e30024 (2012).

[8] M. Zgirski et al., Evidence for Long-Lived Quasiparticles Trapped in Superconducting Point Contacts. Phys. Rev. Lett. **106**, 257003 (2011).

[9] M. A. Despósito and A. Levy Yeyati, Controlled dephasing of Andreev states in superconducting quantum point contacts. Phys. Rev. B **64**, 140511(R) (2001).

[10] E. Pinsolle, A. Rousseau, C. Lupien, B. Reulet, Direct measurement of the electron energy relaxation dynamics in metallic wires, Phys. Rev. Lett. **116**, 236601 (2016).

[11] D.G. Olivares, L. Bretheau, .Ç.O. Girit, H. Pothier, C. Urbina, and A. Levy Yeyati, Dynamics of quasiparticle trapping in Andreev levels, Phys. Rev. B **89**, 104504 (2014).

[12] M. Boissonneault, J. M. Gambetta, and A. Blais, Purcell effect with microwave drive: Suppression of qubit relaxation rate, Phys. Rev. A **77**, 060305(R) (2008).

[13] A. Zazunov, A. Brunetti, A. Levy Yeyati and R. Egger, Quasiparticle trapping, Andreev level population dynamics, and charge imbalance in superconducting weak links, Phys. Rev. B. **90**, 104508 (2014).